Interpreting STEREO observations of 3D CMEs
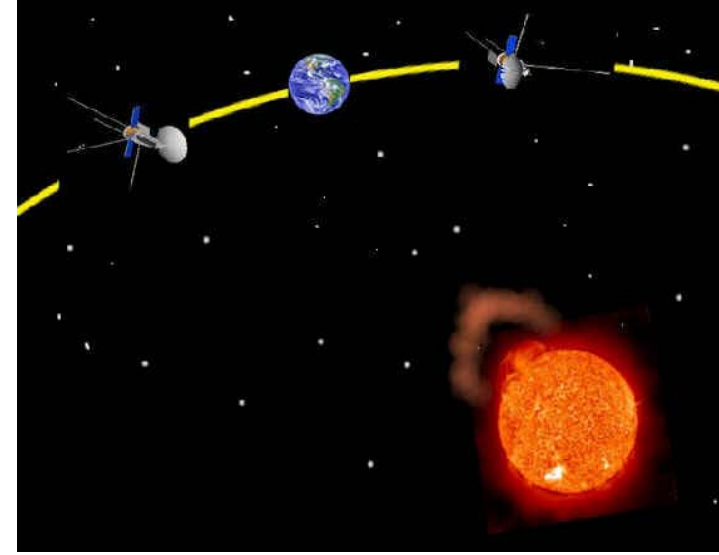
Sarah Gibson, Joan Burkepile, and Giuliana de Toma

Paul Charbonneau

HAO/NCAR

Outline and motivation

- **The CME is a 3D beast**

  STEREO will provide multiple simultaneous views

- **Data analysis tools for STEREO analysis need to be developed**

  Our approach: forward modeling

- **Requires an efficient means of searching model space**

  Genetic algorithms

- **3D density models of CME**

  Simple "ice cream cone" model
  Variation on full 3d MHD model (*Gibson and Low, 1996*)
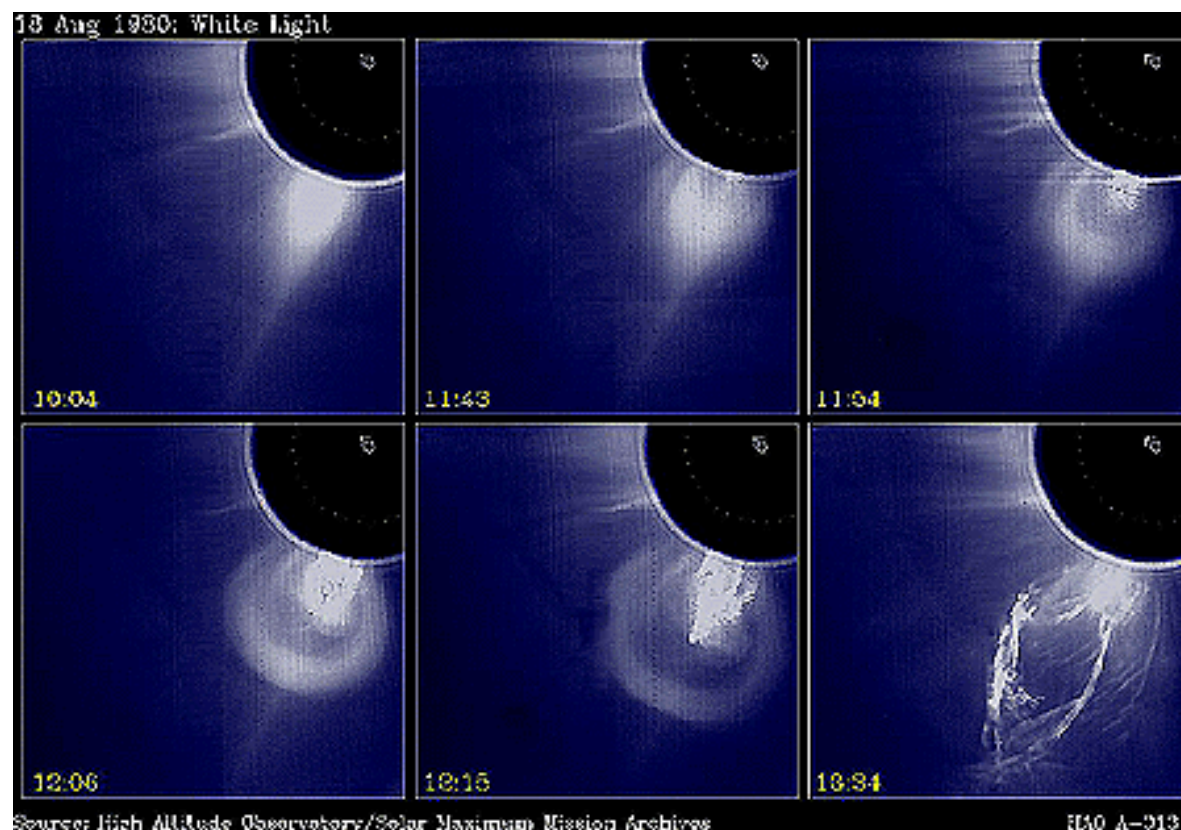
- **Conclusions**

Coronal Mass Ejections

QuickTime™ and a
Sorenson Video decompressor
are needed to see this picture.

- Episodic expulsions of plasma $>\sim 10^{15}$ grams each
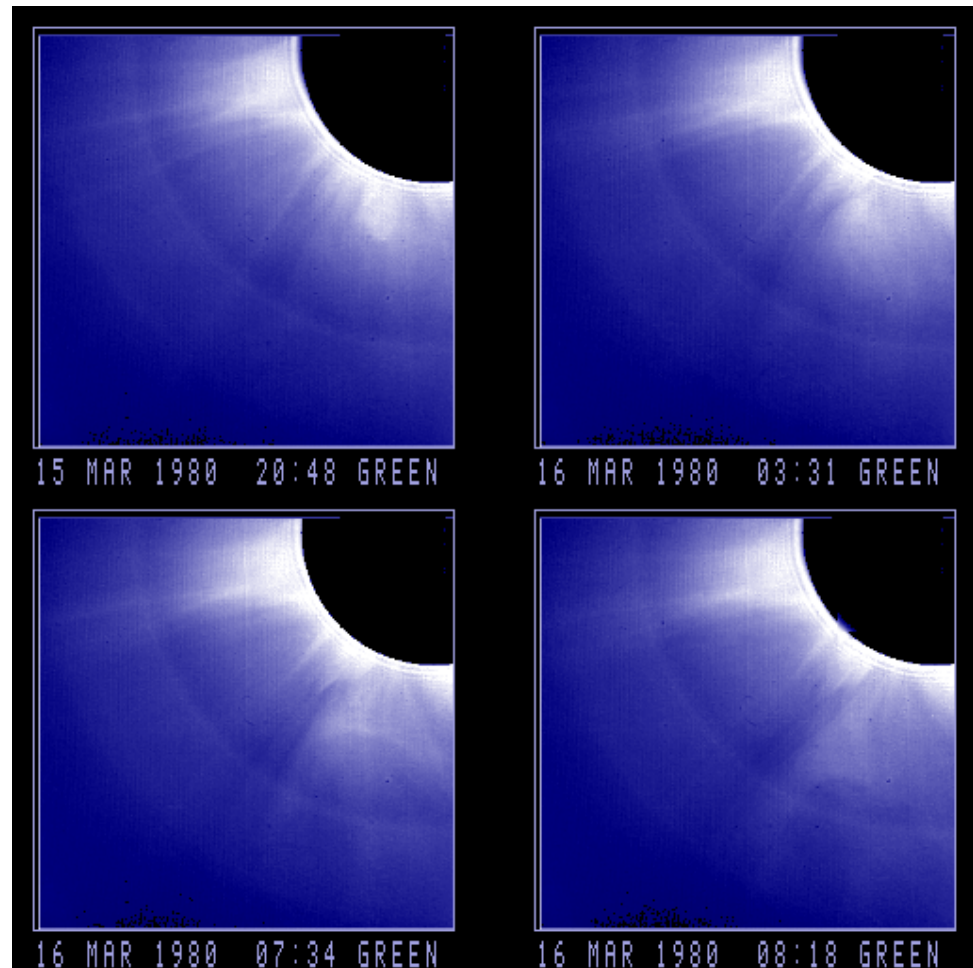
White light CMEs

- ## 3-Part structure

QuickTime™ and a
GIF decompressor
are needed to see this picture.

White light CMEs

- U-shape

White light CMEs

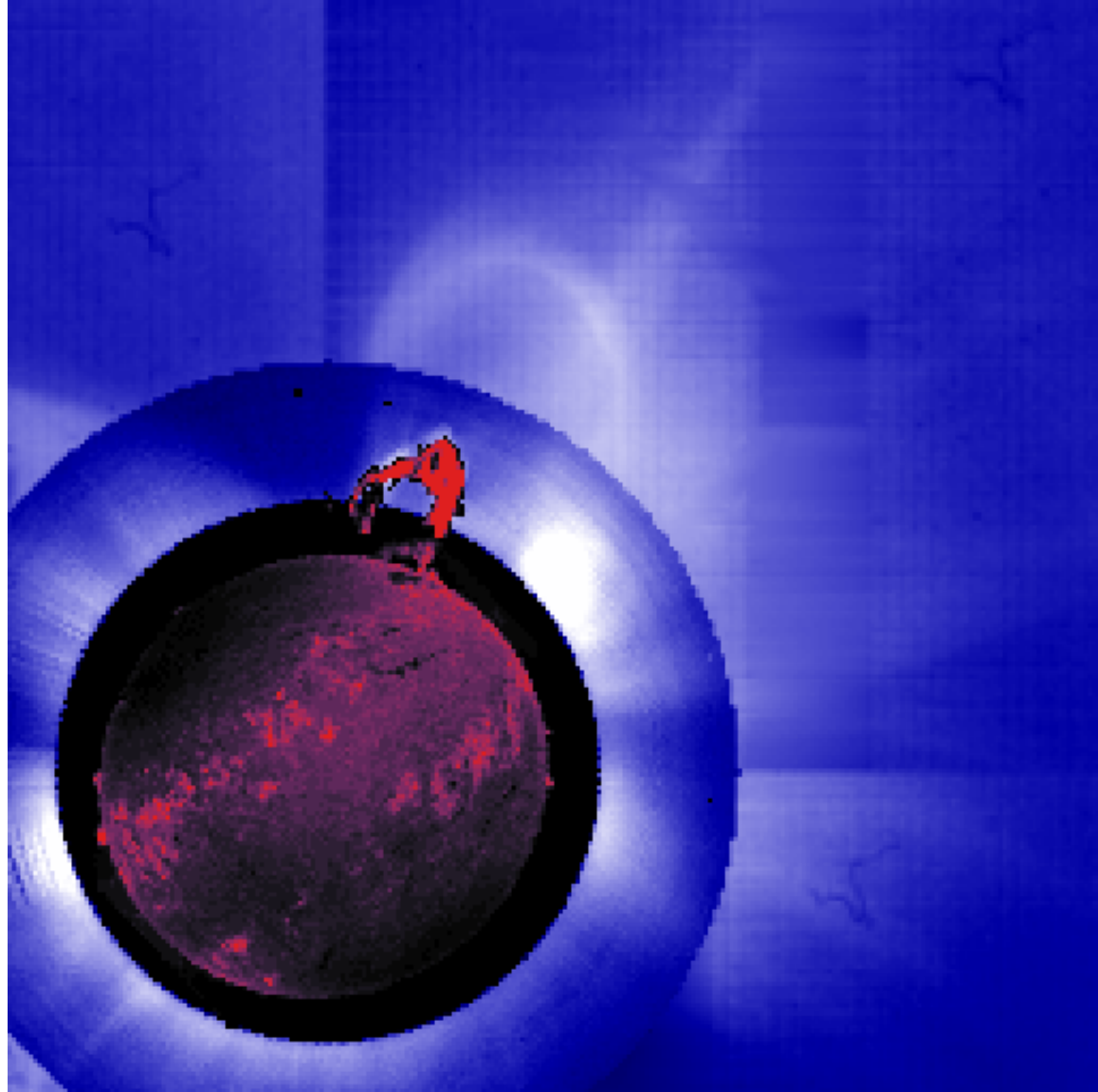- Halo

QuickTime™ and a
Video decompressor
are needed to see this picture.
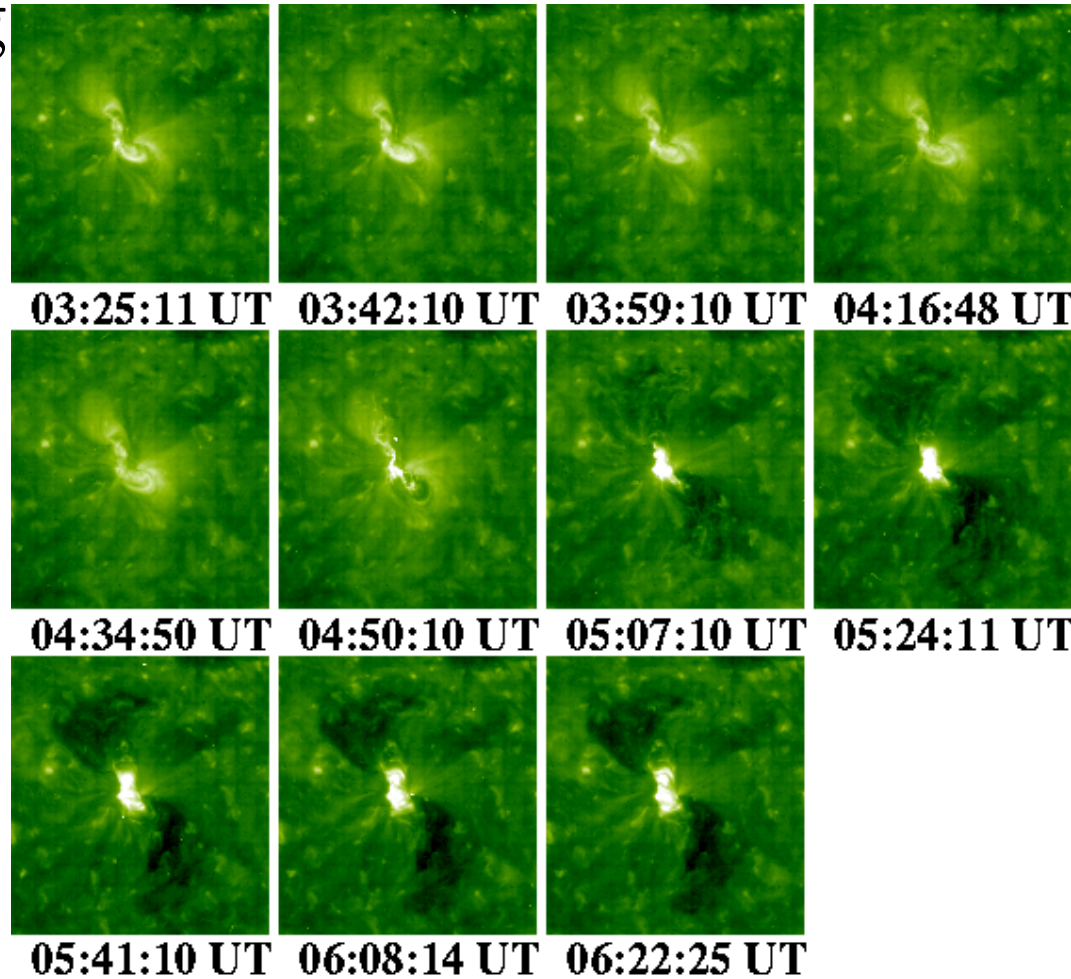
CMEs (and associated phenomena) in emission

- "Cold" emission ~ 10^4 K -- H-alpha): prominence eruption

QuickTime™ and a
GIF decompressor
are needed to see this picture.
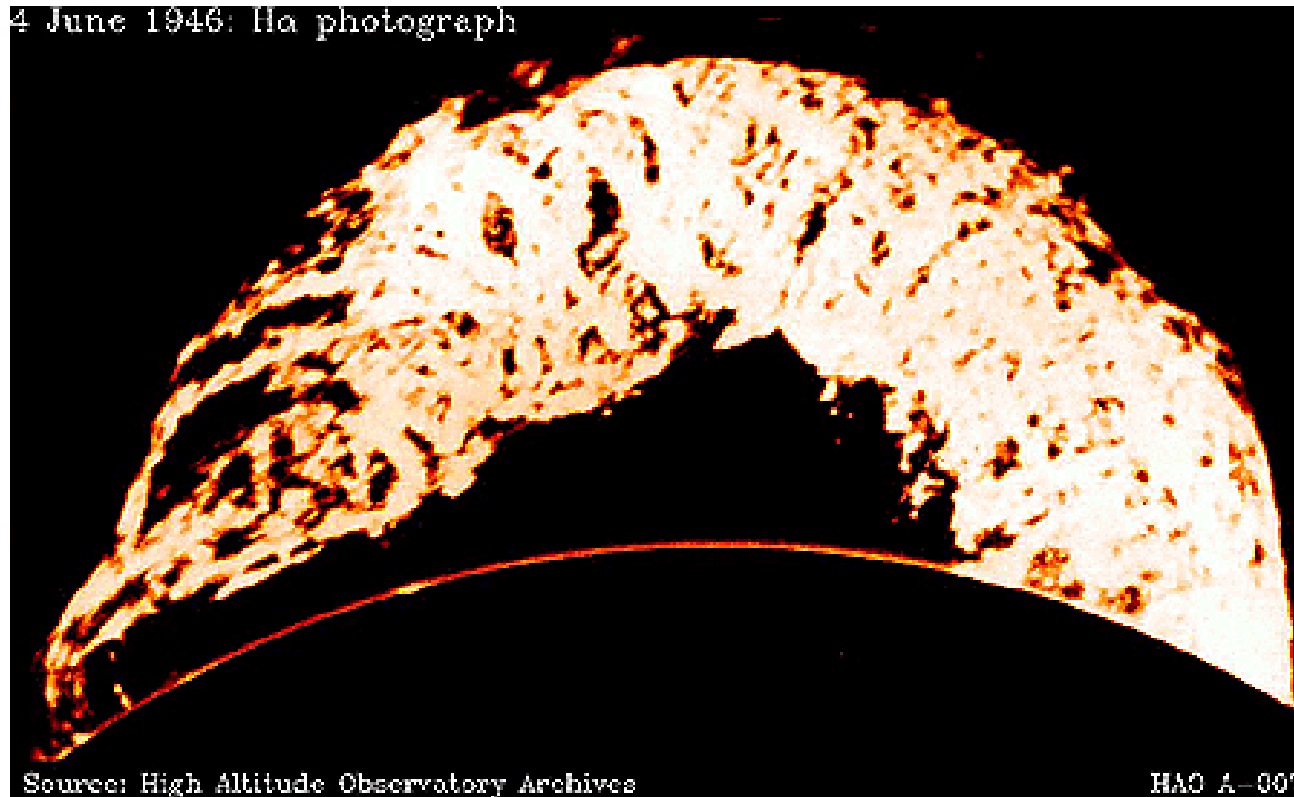
CMEs (and associated phenomena) in emission

- Hot emission (~ 10^6 K -- FeXII): Dimming

QuickTime™ and a
decompressor
are needed to see this picture.

03:25:11 UT 03:42:10 UT 03:59:10 UT 04:16:48 UT

04:34:50 UT 04:50:10 UT 05:07:10 UT 05:24:11 UT

05:41:10 UT 06:08:14 UT 06:22:25 UT

CMEs have a complex, 3D density and temperature structure.

4 June 1946: Hα photograph

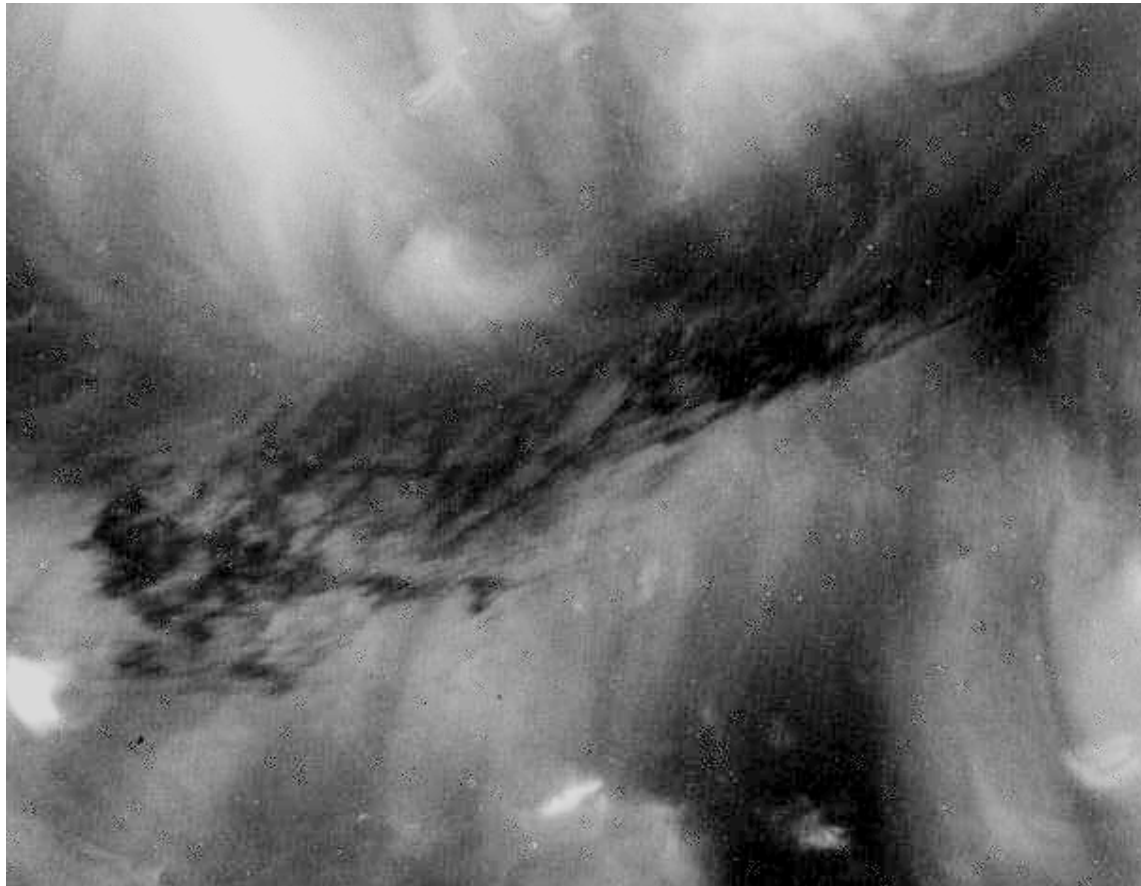Source: High Altitude Observatory Archives

HAO A-007

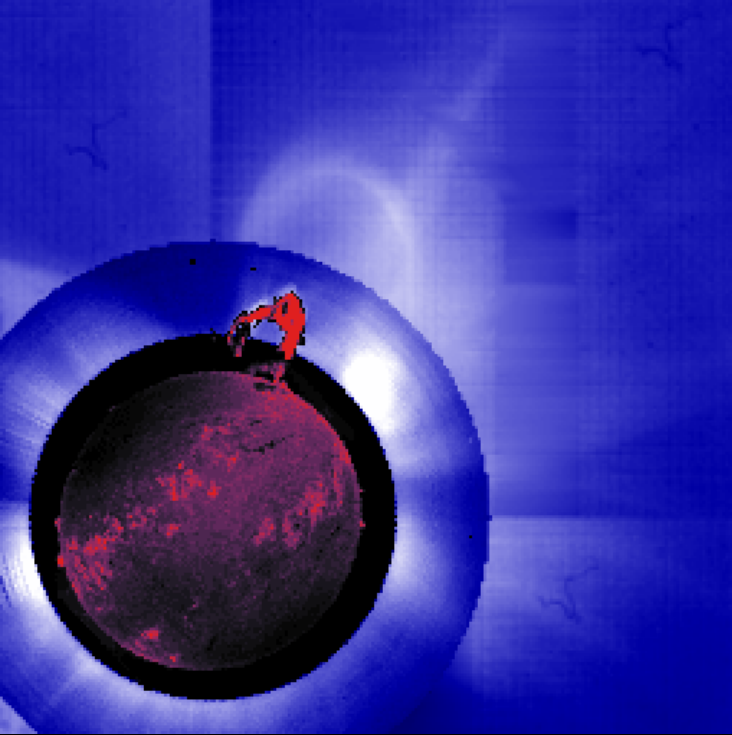3D complexity is well illustrated by twisted structures associated with CMES

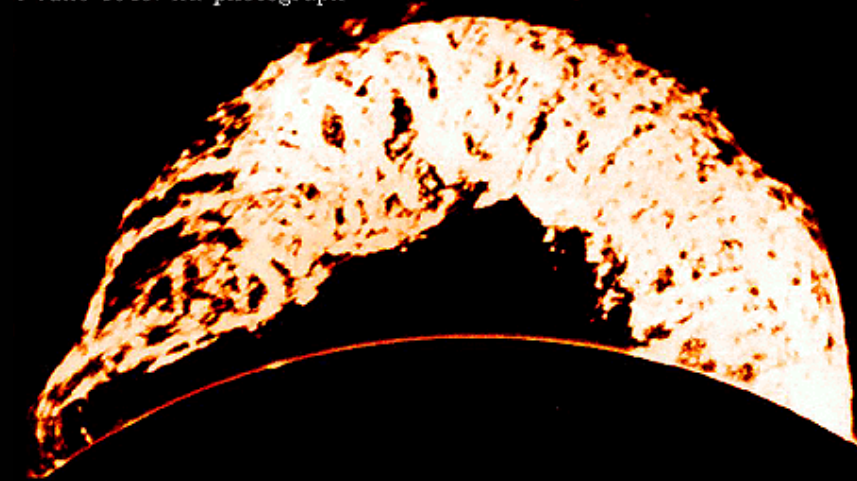# Apparent twist in white light CME core

1998/06/02 13:31:06
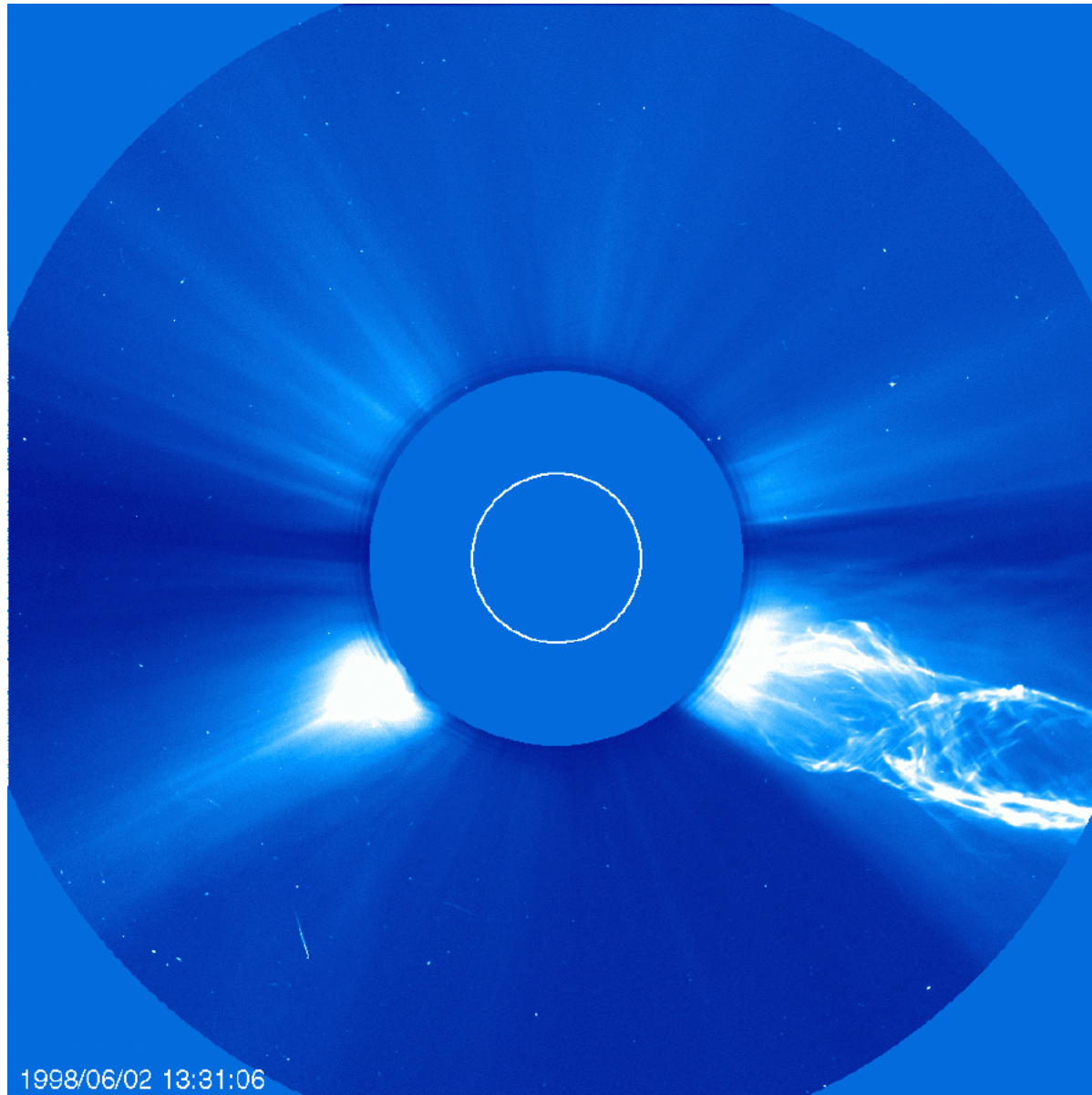
Apparent braided type structure seen in filament (projected on solar disk)

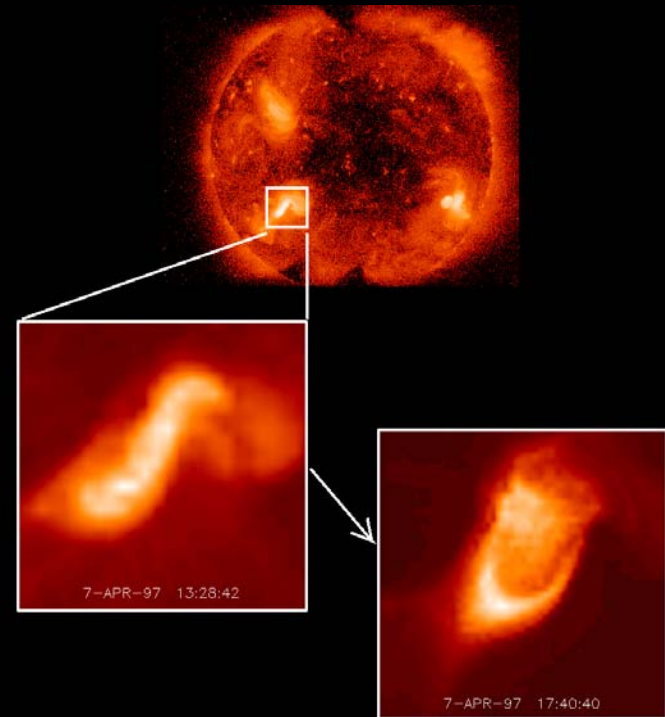# The many faces of the CME

4 June 1946: Hα photograph

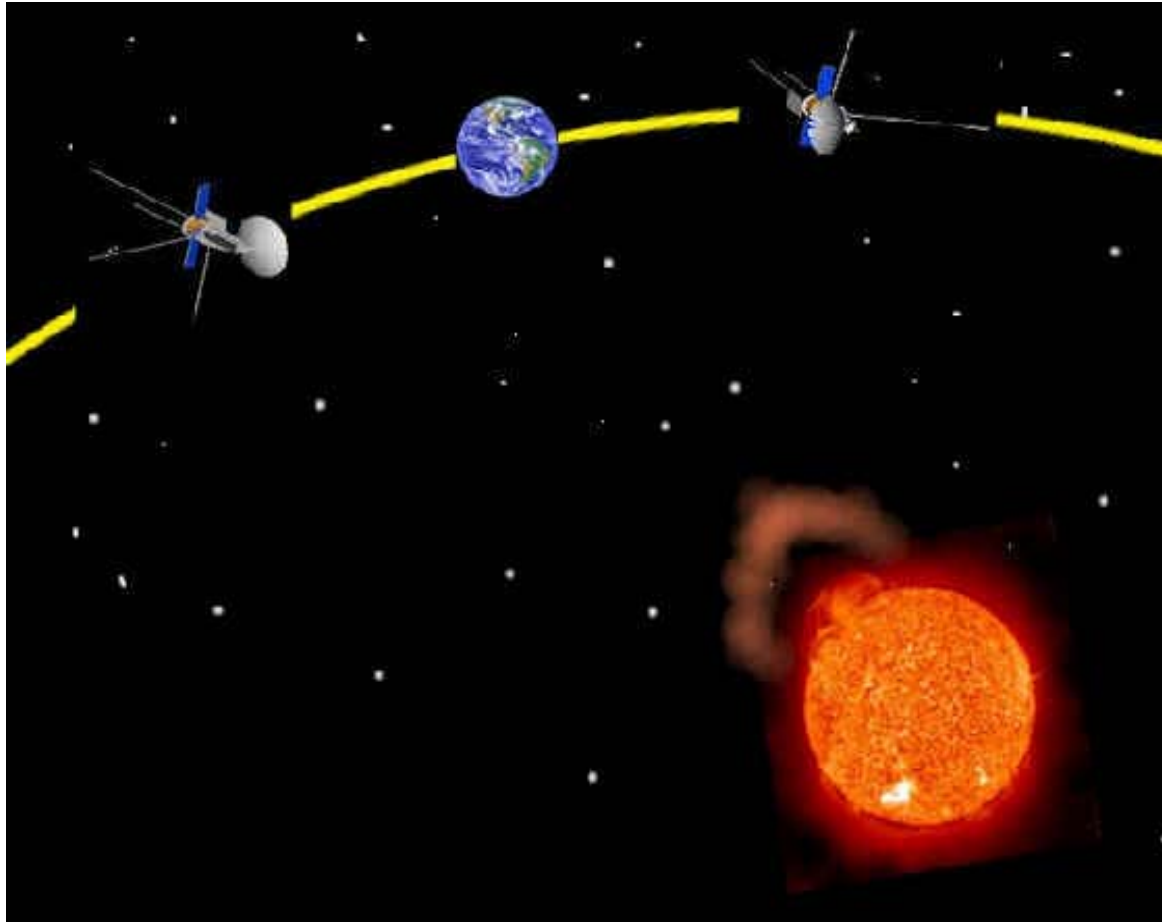Source: High Altitude Observatory Archives   HAO A-007

7-APR-97 13:28:42

7-APR-97 17:40:40

STEREO mission

The STEREO mission setup: two identical spacecraft with identical instrument complements will move in opposite directions away from the Sun-Earth line. Thus, the instruments will provide 2 of 3 observing angles, with the third being covered by instruments viewing along the Sun-Earth line. The SECCHI component of the STEREO mission will include a suite of remote sensing instruments including two white light coronagraphs (COR1 and COR2) and an EUV imager (EUV1), known collectively as the Sun Centered Imaging Package (SCIP), as well as a Heliospheric Imager (HI).

Technique: Genetic Algorithm Based Forward Method

Why use a model?

   For the dynamic CME, tomographic methods are of limited use

   Parameterized model allows 3-d fit to observations (assuming a good model)

How can models be related to observables?

   We will consider density models <---> white light coronagraph observations

$$pB(r,\theta,\phi) = \int N_e(r,\theta,\phi) \cdot)$$

pB = polarized brightness
N_e = electron number density
.) = Thomson scattering

Technique: Genetic Algorithm Based Forward Method

$$pB(r,\theta,\phi) = \int N_e(r,\theta,\phi) \cdot \quad)$$

Inverse method:

Given a parametrized CME density model, the (matrix) integral equation can be inverted with respect to Brightness (B) or polarized Brightness (pB) observations to yield the best model parameters (if, as is usual, the model is nonlinear in its parameters, this requires for example iterative stepping in the direction of *steepest descent*).

Forward method:

Density is specified from a CME model, and integrated along the line of sight to yield B or pB intensity. This is directly compared to observations to determine a goodness of fit. If parameter space is sufficiently searched, the best fit solution(s) can be determined.

Technique: Genetic Algorithm Based Forward Method
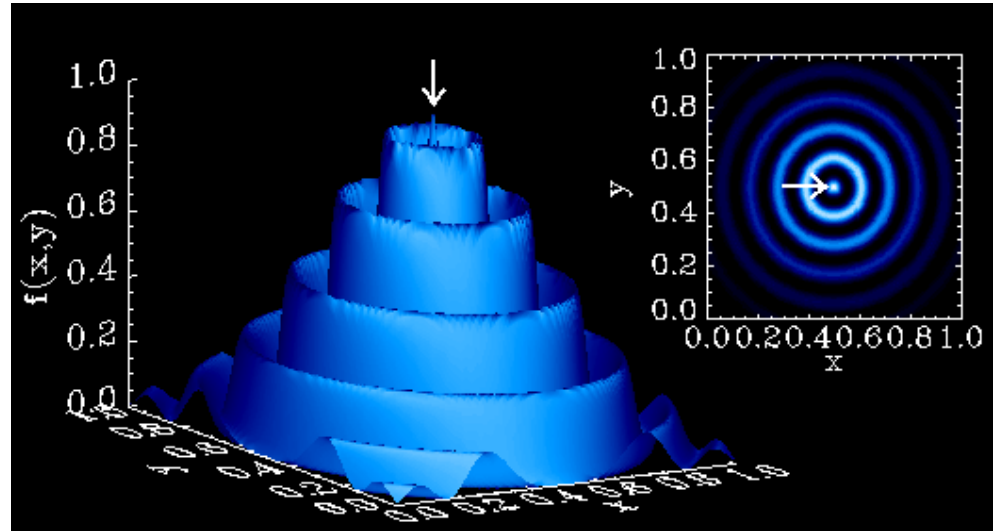
Why use a forward method?

3-D coronal inverse problem fundamentally ill-posed: **observational nonuniqueness** and **model degeneracy**

A forward technique that thoroughly searches parameter space allows **observational nonuniqueness** and **model parameter degeneracy** to be mapped out and **quantified as global error bars**

Additional observational information, such as white light observations along the three STEREO lines of sight or on-disk observations pinpointing the CME location and/or angular extent, **can easily be incorporated**

Error amplification is intrinsic to nonlinear inversion of integral equations

Error amplification is avoided by using the forward method

Technique: Genetic Algorithm Based Forward Method

Why use genetic algorithms?

Need a **global optimizer** to span parameter space

- Grid search or Monte Carlo method: number of evaluations $\sim N_{res}^{npar}$

Example: to randomly generate METHINKS IT IS A WEASEL $\sim$ **10^{33} iterations**

Introduce **natural selection** (that is, choose a "population" of 10 random choices of 23 letters, select the one that best matches target sentence, make new population of 10 duplicates each with one letter randomly toggled, continue): **1240 iterations**

decompressor
are needed to see this picture.

Like the above example, genetic algorithms contain elements of **inheritance** (which makes search more **efficient**) and **mutation** (which helps **avoid local minima**)

Moreover, G.A. parameter sets (the members of the population) are coded into chromosome-inspired strings: pairs of these are spliced together via a **crossover** operation, allowing some of the next population ("children") the possibility of possessing the best of both "parents". This both **increases efficiency** and allows a **broader exploration of parameter space**.

See Paul Charbonneau's "pikaia" page for more information and a public domain genetic algorithm routine:
http://www.hao.ucar.edu/public/research/si/pikaia/pikaia.html

Technique: Genetic Algorithm Based Forward Method

How are genetic algorithms implemented?

Assuming a problem where a set of model parameters determines an observable property, start with a randomly generated "population" of parameter sets

1. Evaluate the goodness of fit (``fitness") of each member of the current population (through a chi square measure with the data, for example).
2. Select pairs of solutions (``parents") from the current population, with the probability of a given solution being selected made proportional to that solution's fitness.
3. Breed the two solutions selected in (2) and produce two new solutions (``offspring"), introducing elements of "crossover" and "mutation".
4. Repeat steps (2)-(3) until the number of offspring produced equals the number of individuals in the current population.
5. Use the new population of offspring to replace the old population.
6. Repeat steps (1) through (5) until some termination criterion is satisfied (e.g., the best solution of the current population reaches a goodness of fit exceeding some preset value).
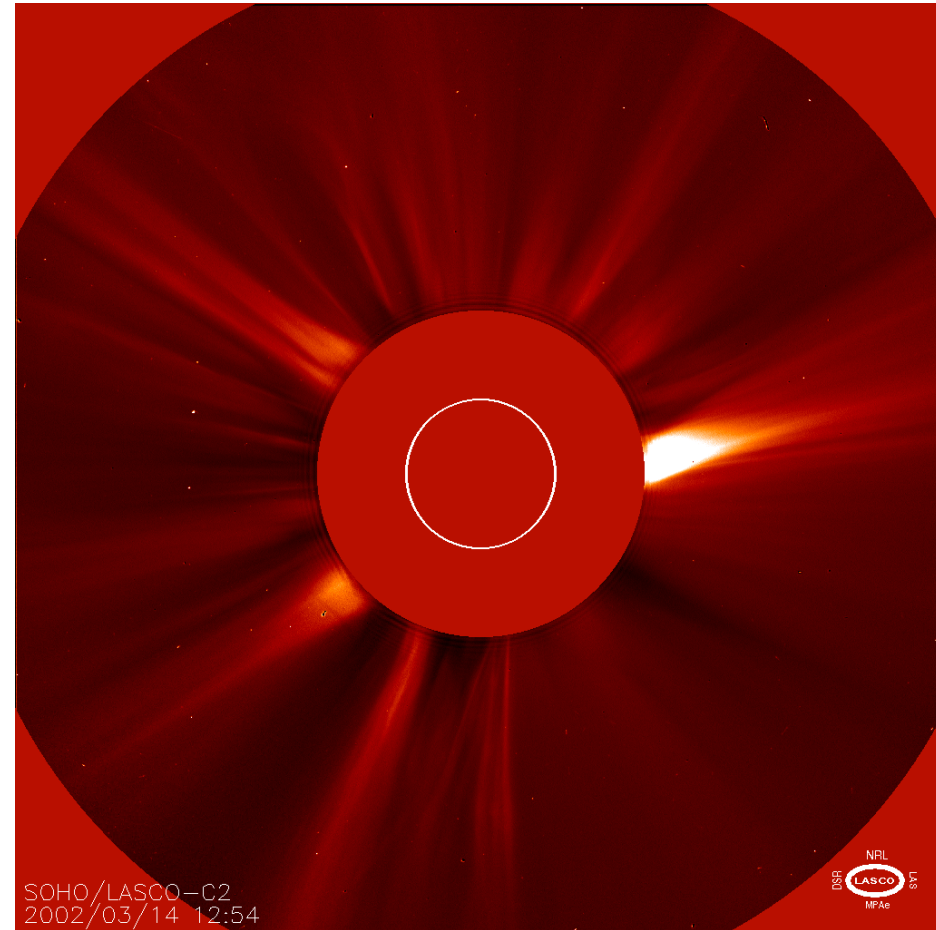
Density models: 1) "Ice cream cone"
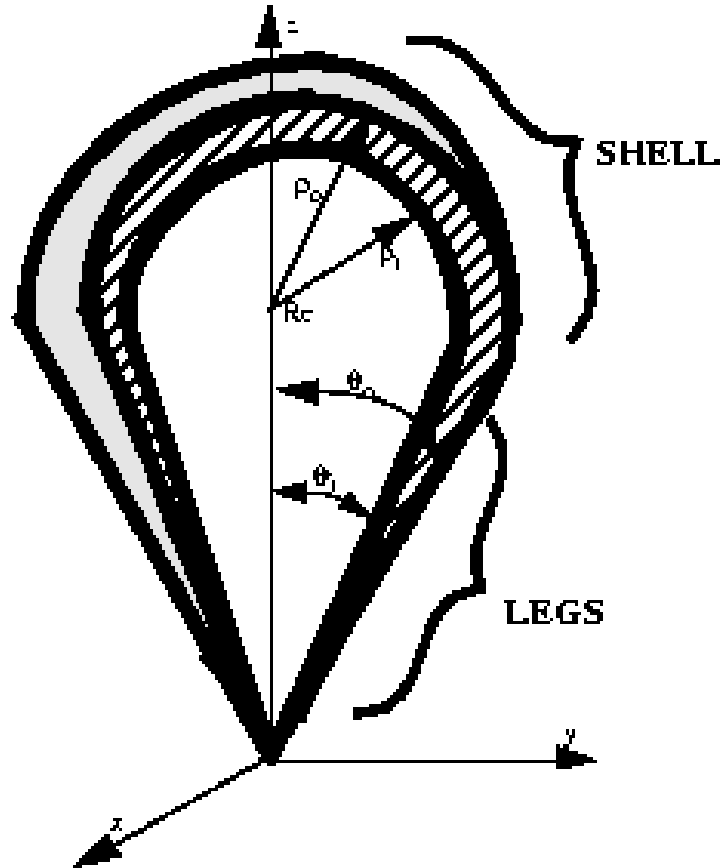
When projected in 2-D, the basic 3-D "ice cream cone" model captures the commonly observed white-light loop-cavity morphology.
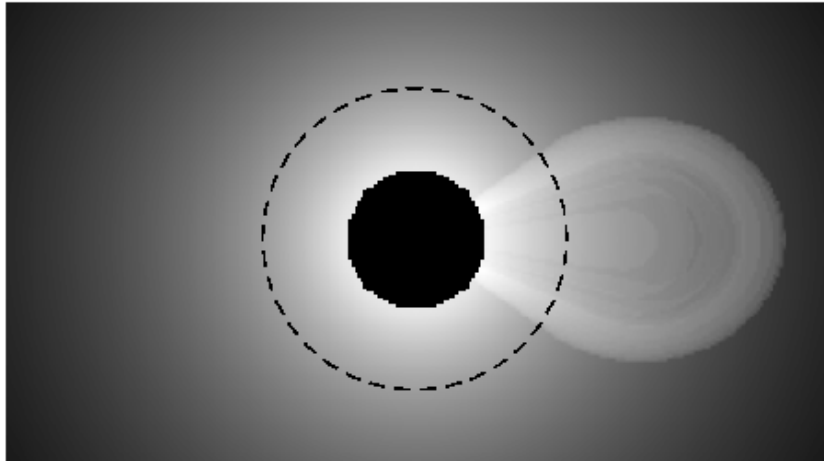
White light coronal observations

QuickTime™ and a
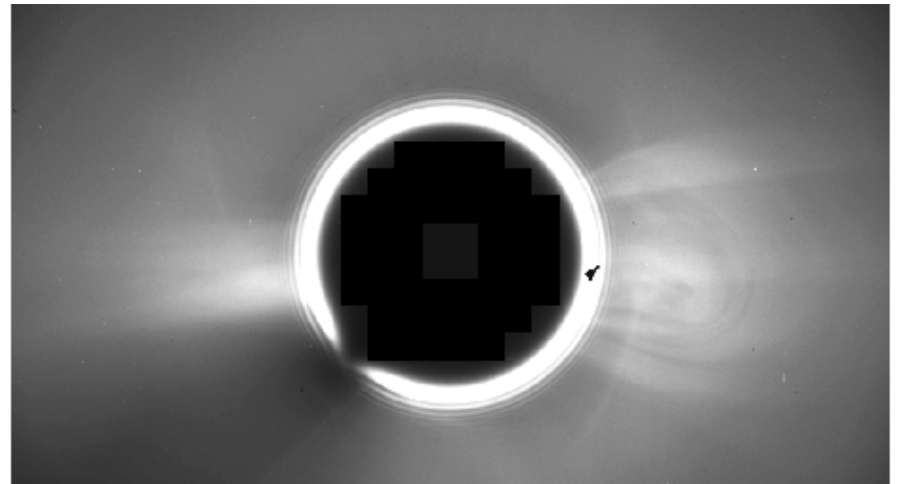decompressor
are needed to see this picture.

March 14, 2002 white light coronagraph images, MLSO/Mark 4 (left) and LASCO/C2 (right).

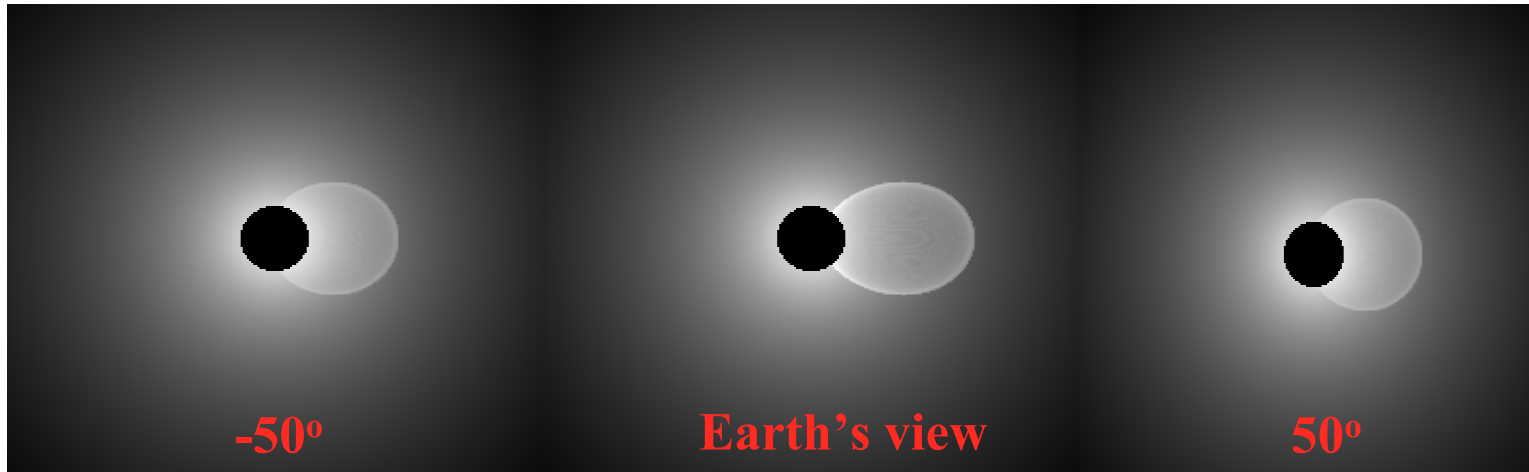# Density models: 1) "Ice cream cone"

"Ice cream cone" **model** brightness

LASCO/C2 **observed** brightness

Density models: 1) "Ice cream cone"

Case 1: CME centered at west limb (90°), $\alpha_i=30^o$, $\alpha_o=35^o$, $R_c=4$ R_{sun}

Case 2: CME centered at 45°, shell density double Case 1, $\alpha_i=50^o$, $\alpha_o=55^o$, $R_c=2.7$ R_{sun}

Density models: 2) Modified MHD model
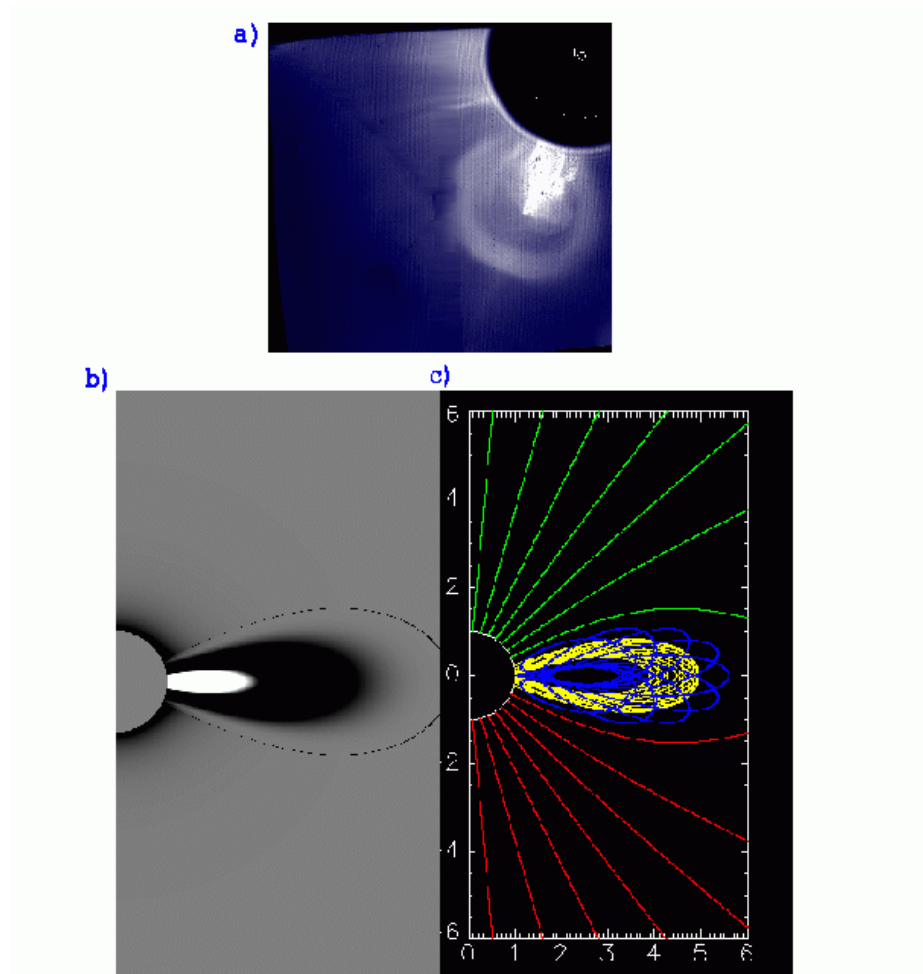
Another way of obtaining a 3-part loop-cavity-core structure is by using a 3-D MHD model of the CME (*Gibson and Low, 1998*). In this case, the 3-part morphology of the density distribution is physically defined by the magnetic field topology.

Theoretical description of CMEs

Need to solve ideal magnetohydrodynamic (MHD) equations in order to self-consistently describe the magnetic field and its interaction with the coronal plasma.

$$\rho\left[\frac{\partial \boldsymbol{v}}{\partial t} + (\boldsymbol{v} \cdot \boldsymbol{\nabla})v\right] = \frac{1}{4\pi}\left(\boldsymbol{\nabla} \times \boldsymbol{B}\right) \times \boldsymbol{B} - \boldsymbol{\nabla}p - \rho\frac{GM}{r^2}\hat{\boldsymbol{r}}, \quad (1)$$

$$\frac{\partial \rho}{\partial t} + \boldsymbol{\nabla} \cdot (\rho \boldsymbol{v}) = 0, \qquad (2)$$

$$\frac{\partial \boldsymbol{B}}{\partial t} = \boldsymbol{\nabla} \times (\boldsymbol{v} \times \boldsymbol{B}), \qquad (3)$$

$$\frac{\partial}{\partial t}\left(p\rho^{-\gamma}\right) + (\boldsymbol{v} \cdot \boldsymbol{\nabla})(p\rho^{-\gamma}) = 0, \qquad (4)$$

Model complexity must be sufficient to reproduce the essential observational complexities.

What are spheromaks?

Spherical, closed magnetic system containing comparable toroidal and poloidal magnetic fields generated by currents within the structure
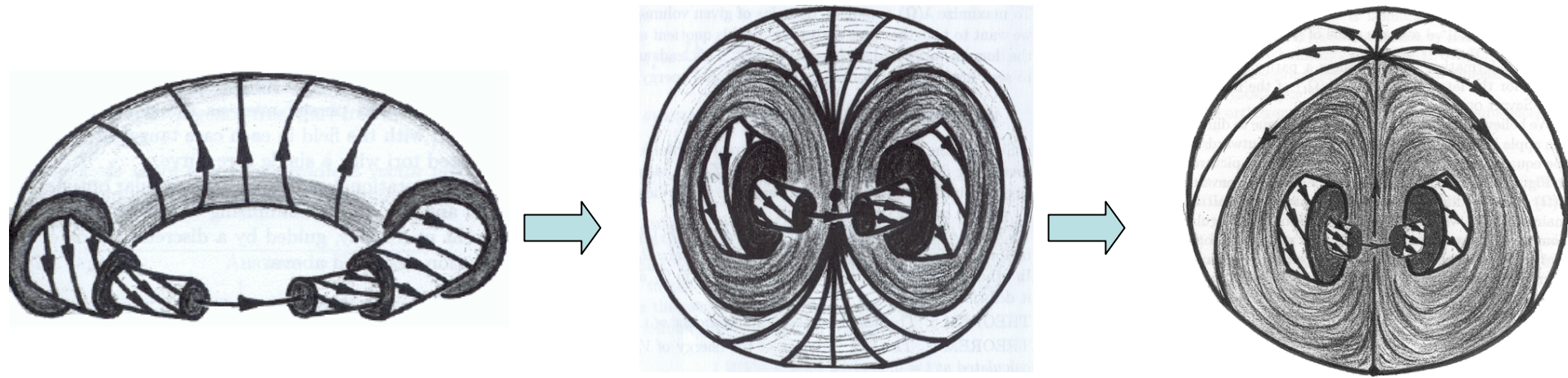
Images from Cantarella, et al., 1999

MHD Model: *Gibson and Low (1998)*
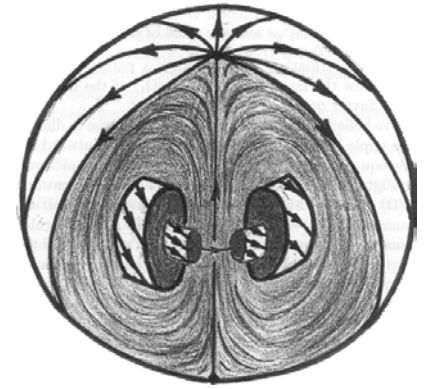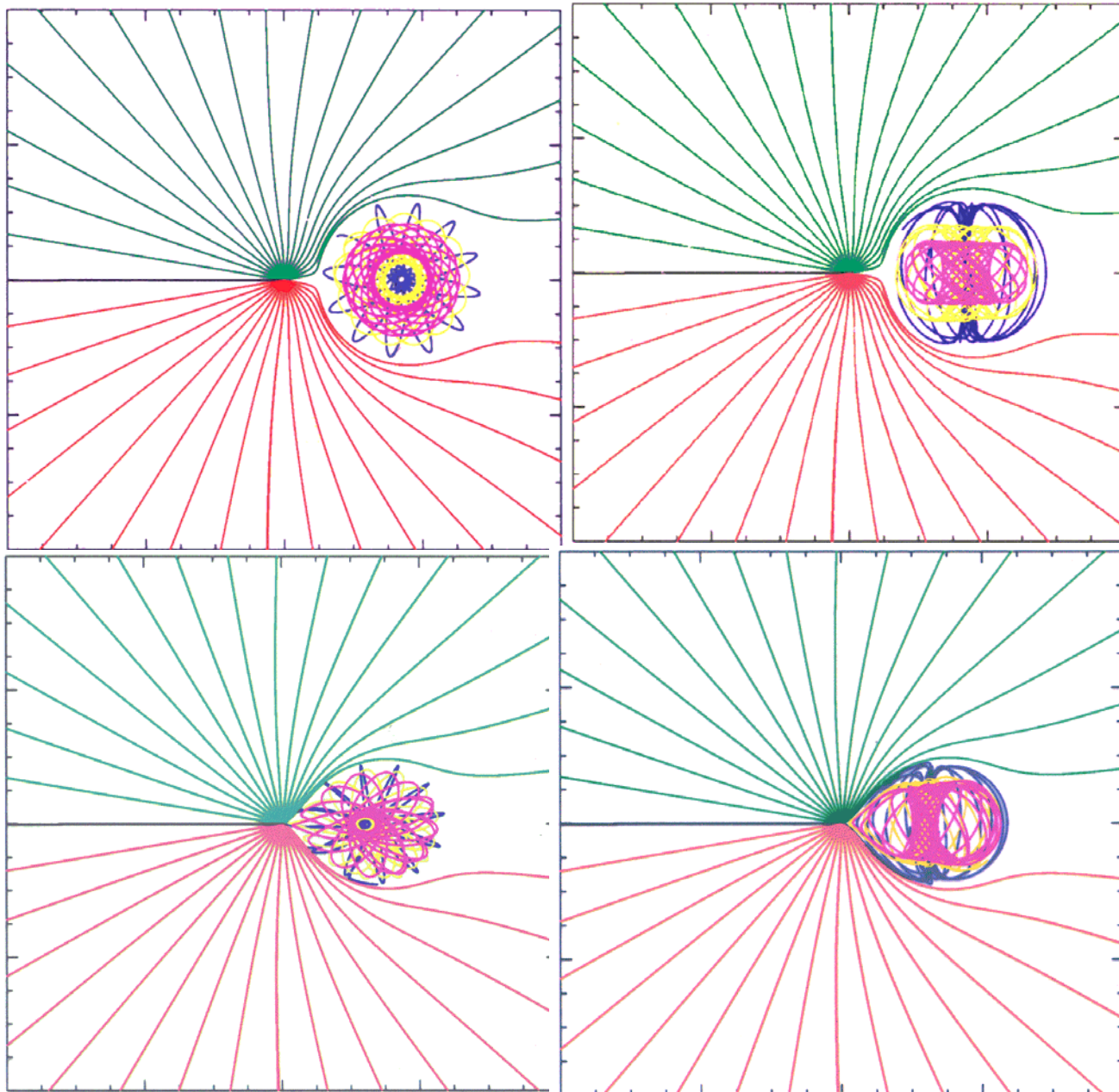
Spheromaks

Why do we use them to model CMEs?

- Circular cross-section: CME observations don't support linear-type structure *(Fisher&Munro, 1984; Webb, 1988; Thompson et al, 1999)*

- Vector magnetogram observations of emerging field orientation and rotation well captured by spheromak model *(Lites et al, 1995)*

- Spheromak model solution yields plasma distributions satisfying a range of observed prominence structures and always yields a bubble-type cavity

Spheromaks represent the spheroidal nature of CMEs better than a linear slinky.

MHD Model Results

Lites and Low, 1996

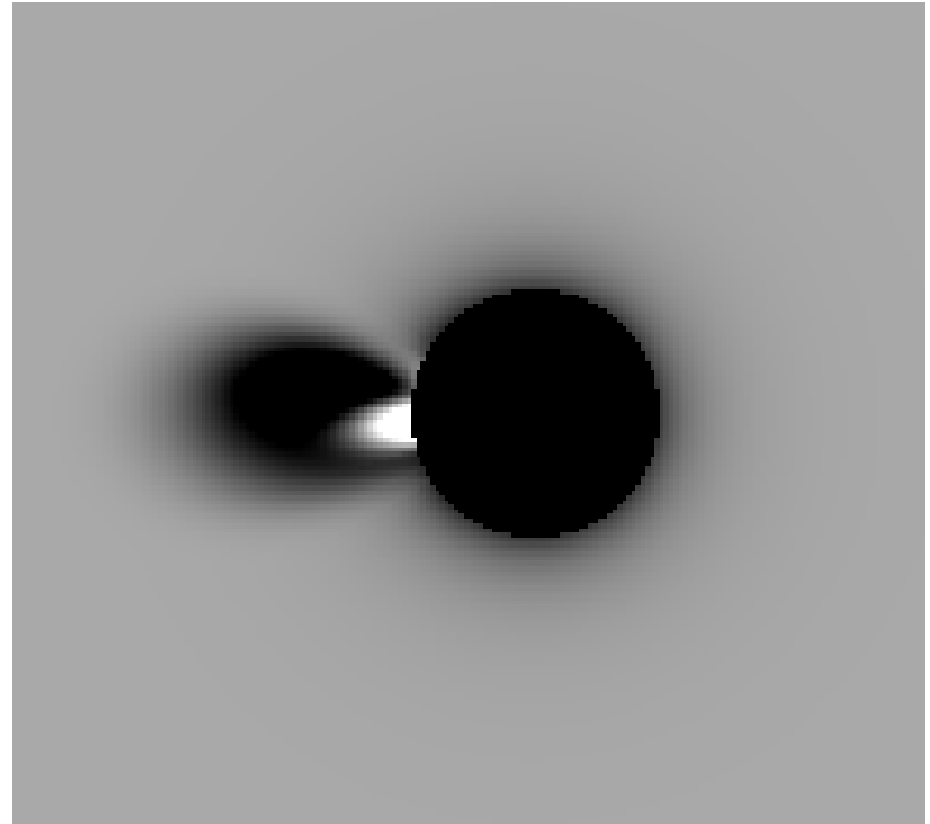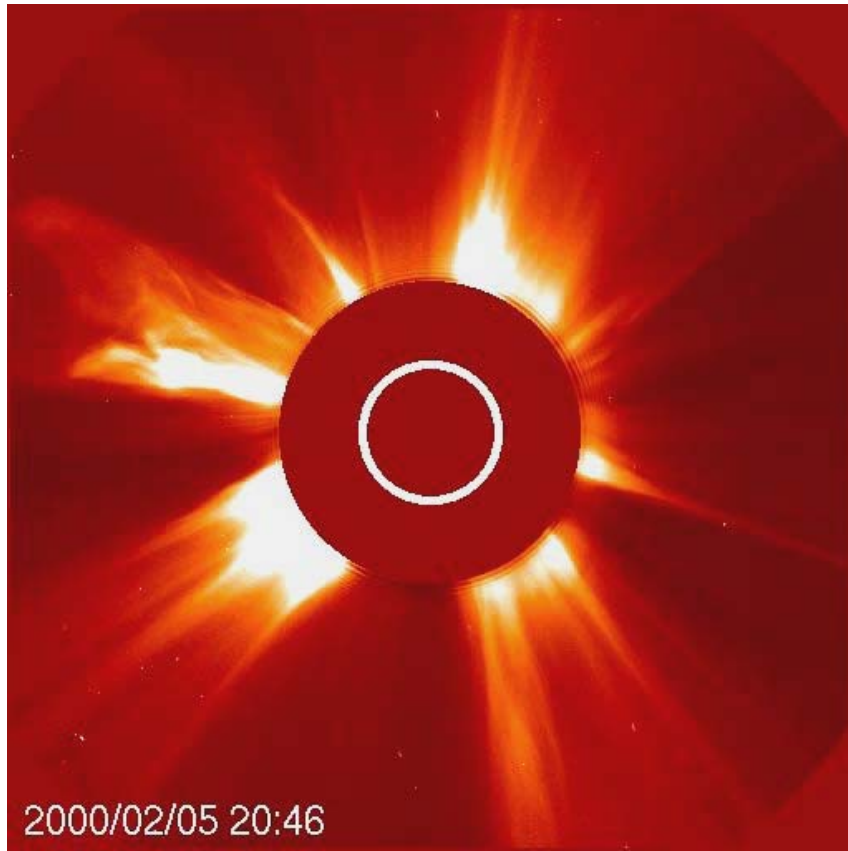# MHD Model predictions at the limb (white light)
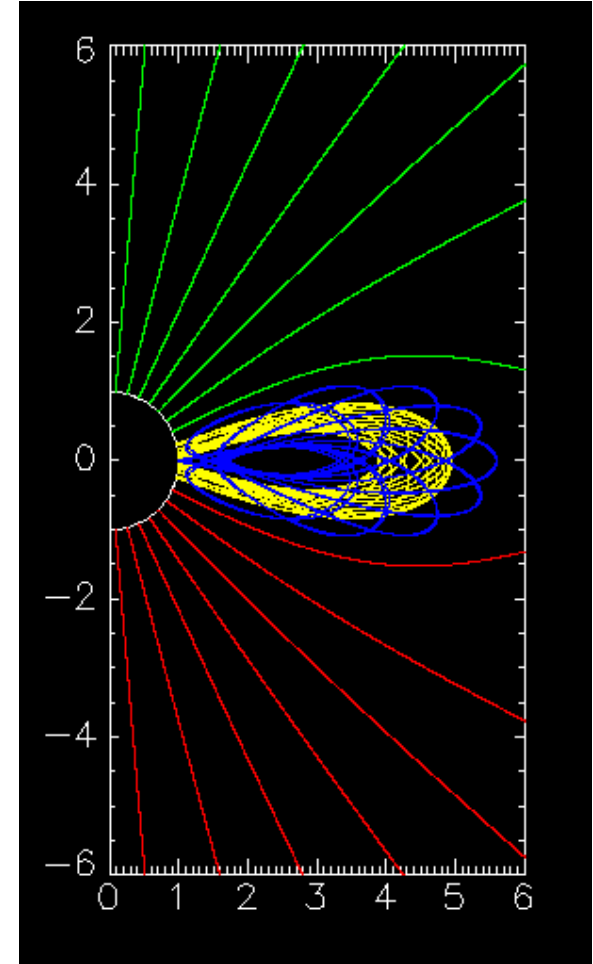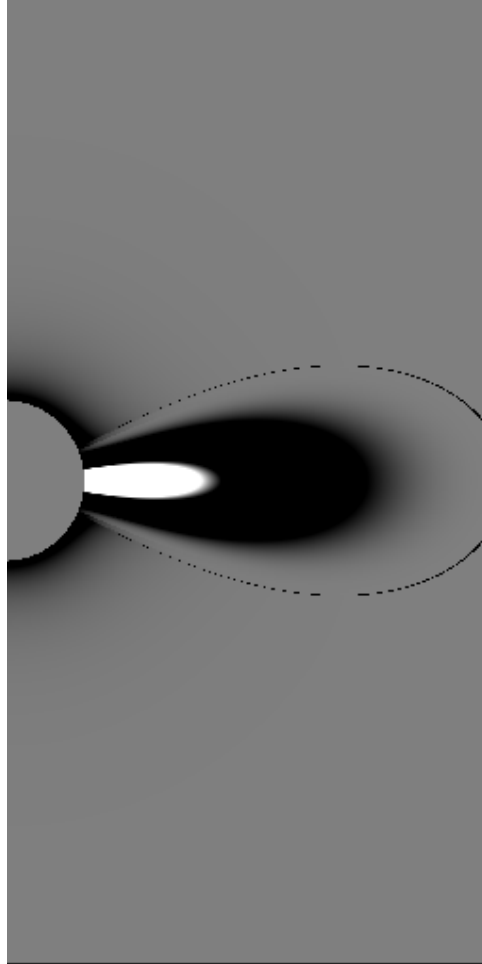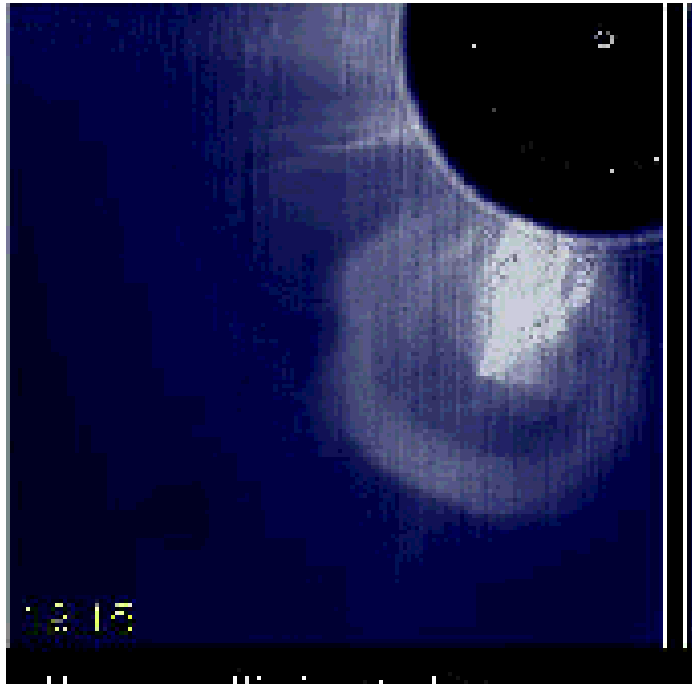
SMM CME observed Aug 18, 1980, Gibson & Low model CME, viewed along CME toroidal axis

MHD Model predictions at the limb (white light)
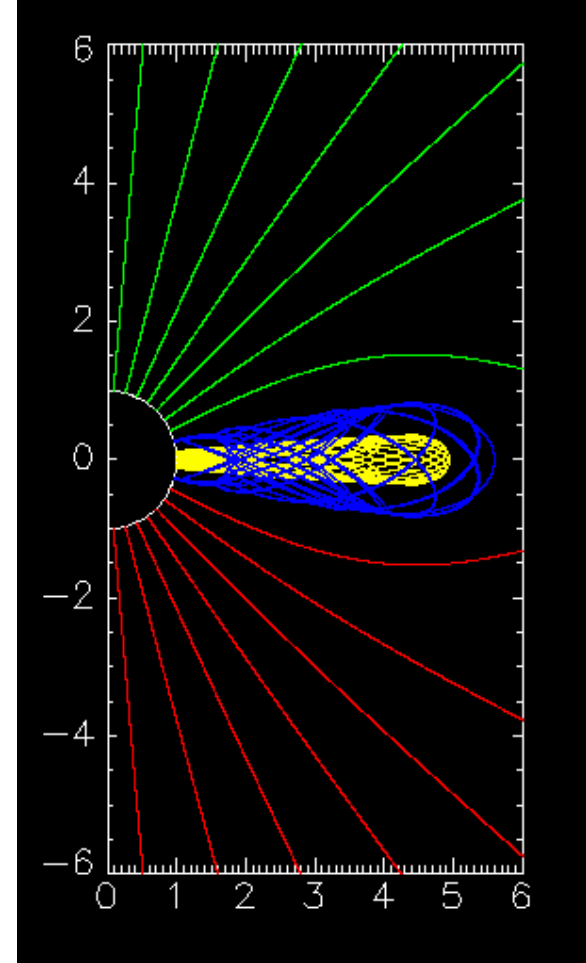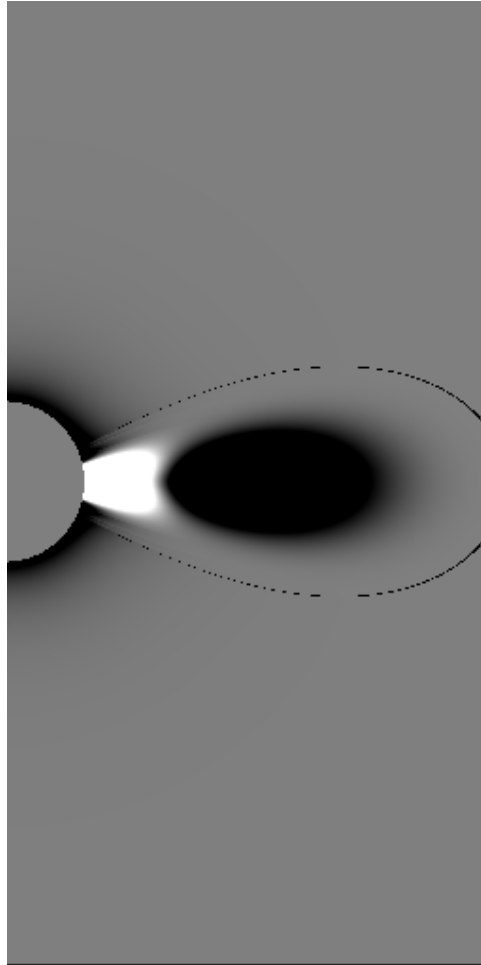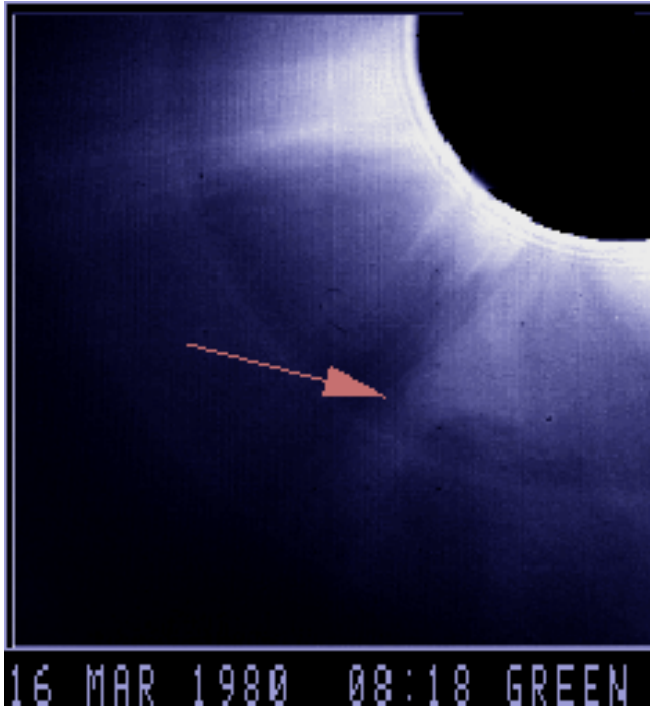
SMM CME observed March 15, 1980, Gibson & Low model CME, viewed perpendicular CME toroidal axis
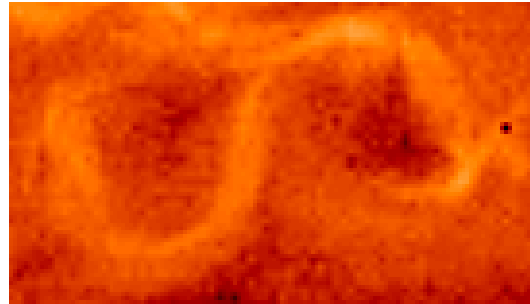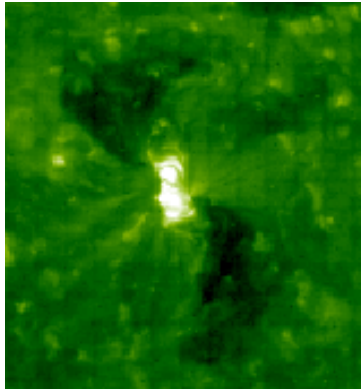
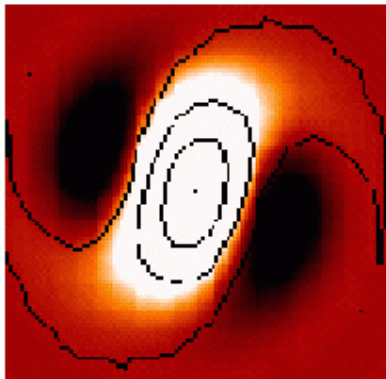# MHD Model predictions at the limb (white light)

2000/02/05 20:46

On-disk behavior - comparison to emission observations

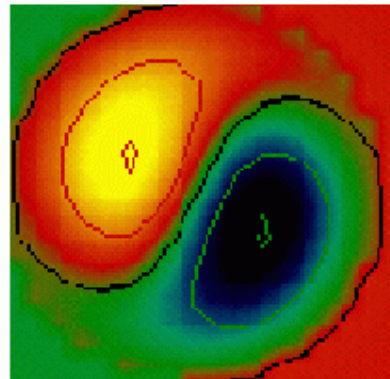(Gibson et al., 1999; Gibson and Low, 2000)
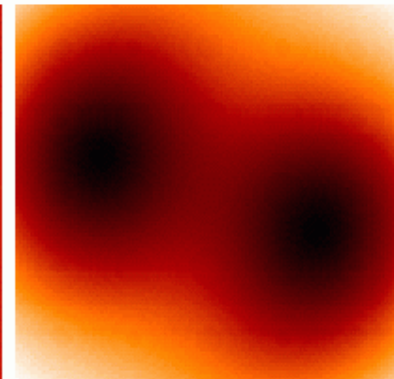
Observations

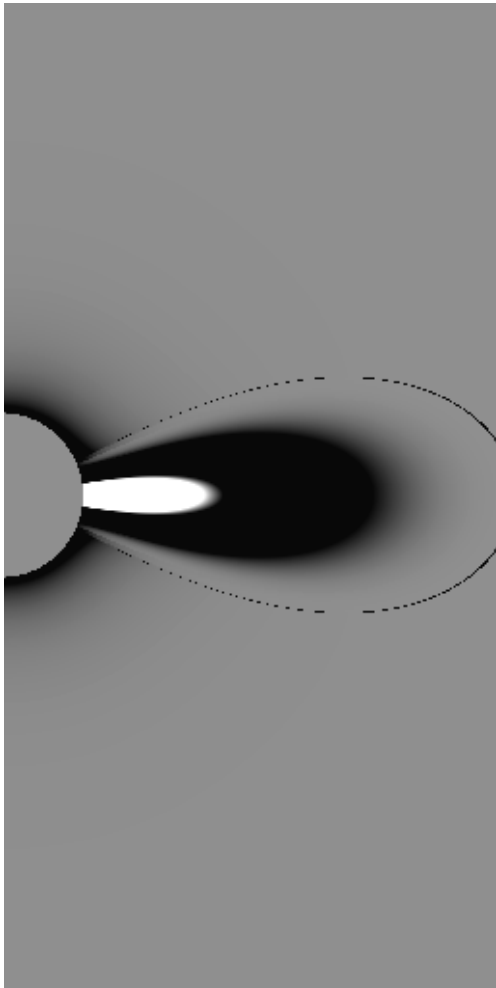**Model (at coronal base)**

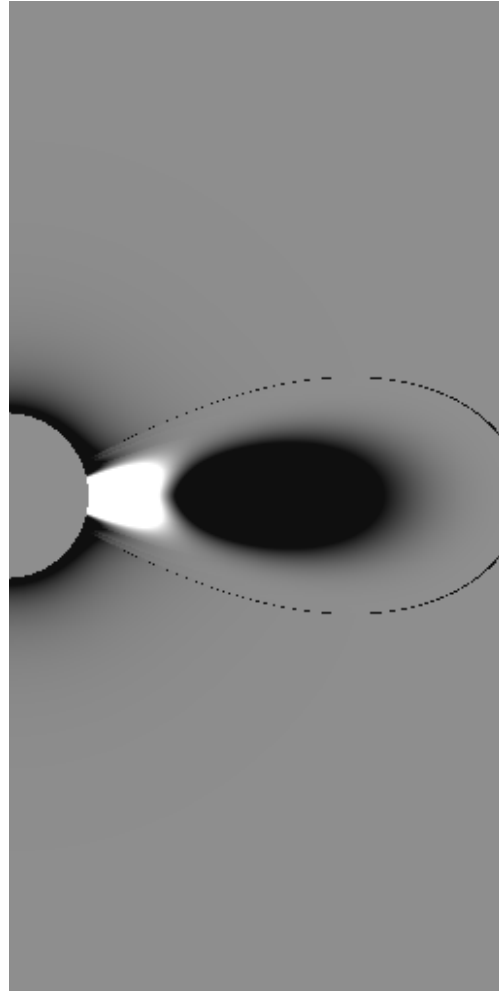| Density | Magnetic field | X-ray emission |

Deconstructing 3D CME observations
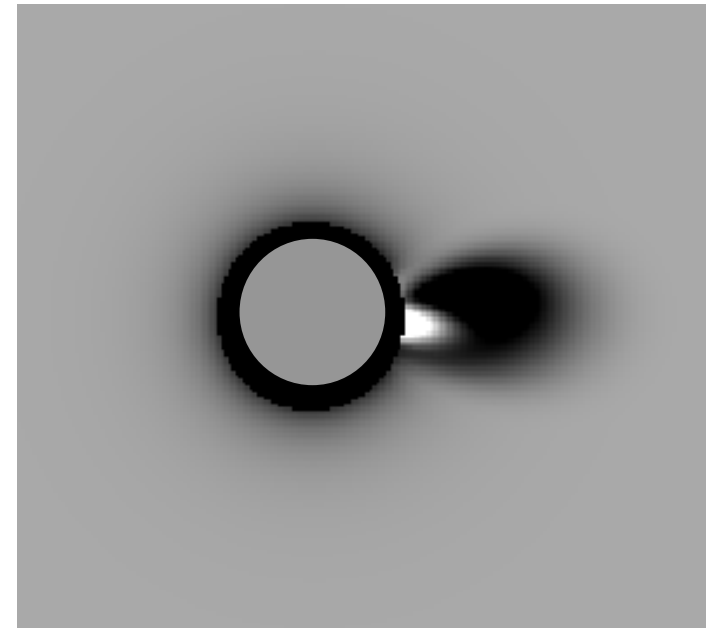
Three views of MHD model CME

Axis along l.o.s

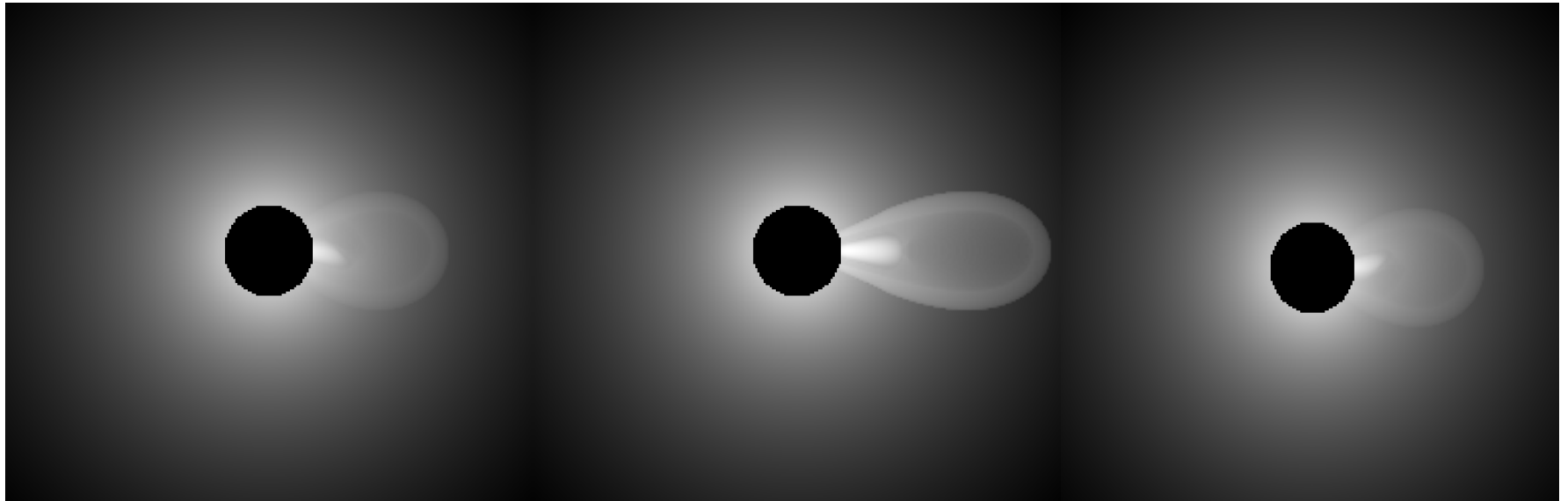Axis perpendicular to l.o.s

Off-limb, and axis at an angle to l.o.s

Density models: 2) Modified MHD model

-50°   **Earth's view**   **50°**

For the purpose of fitting to a range of white light CME observations, we retain the 3-part morphology defined by the Gibson and Low model, but modify the MHD solution to allow for variation of the density profiles within the three region.

Summary and Future Work

Our technique incorporates the following:

- CME density models (ice-cream cone, modified MHD)
- forward method (avoids error amplification, maps out degeneracy)
- genetic algorithm global optimization (efficient and comprehensive)

We plan to develop the technique in anticipation of its application to STEREO observations, and also to immediately use it to investigate existing observations of CMEs. Specifically, we will:

1. Apply our technique to existing data to test and further develop models
2. Set up the code to incorporate STEREO datasets (run sample cases)
3. Include more realistic coronal background models (e.g. *Gibson et al, 1996*)